

UHF band On-Body Wave Propagations and Compact Array Design

Yang Li

Department of Electrical and Computer Engineering
Baylor University
Waco, TX, 76798, USA
Yang_Li1@Baylor.edu

Abstract — On-body wave propagation is investigated for medical frequency bands at 433 MHz and 915 MHz. The paper applies in-situ measurements, full wave numerical simulations, and simplified ground wave and creeping wave theories to calculate the approximate path gain, both along and around a human body. A compact array design, which can be used for potential on-body applications, is also simulated and measured.

Index Terms — Wireless body area network, on-body wave propagation, compact antenna array design

I. INTRODUCTION

Electromagnetic wave propagation and radiation over human body surface have attracted great interests in recent years due to the promising future of wireless body area network (WBAN) in remote health monitoring, battle field communication and personal entertainment, etc. [1]. A WBAN consists of a number of wearable sensors which continuously record physiological data and relay them to a body control unit (e.g. smart phone). A thorough understanding of on-body propagation channels is critical in ensuring reliability and efficiency of WBAN implementation, and can facilitate optimized wearable antenna design which can maximize its radiation into the dominant propagation mechanism.

Driven by this need, researchers have investigated electromagnetic wave propagation along (LOS) and around (NLOS) the human body in WBAN [2, 3]. It was found that: a ground wave is the dominant mechanism for line-of-sight (LOS), near-skin propagation; and a creeping wave contributes most for non-line-of-sight (NLOS), around-torso propagation [4]. The propagation characteristics (i.e., propagation and attenuation constants) of both waves have been extracted and show good agreements with theoretical model [5].

Most of the studies focused on ISM band centered at 2.45 GHz. At high frequency the antenna size is smaller and there is a larger fractional bandwidth leads to a higher data rate. However, the signal attenuates more quickly as the operating frequency increases. Therefore, it is

desirable to utilize low frequency propagation channel (below 1GHz), which results in much lower propagation loss and longer battery life. The antenna size can be optimized with the latest advance of electrically small antenna design. It is also applicable for low data rate (e.g. Heart beats). The wave propagation characteristics and mechanisms remain to be investigated in low UHF frequency bands since the receiving sensor can be in the near field region of the transmitter.

In this paper, we first report on-body EM wave propagations for both line-of-sight (LOS) and non-line-of-sight (NLOS) scenarios at 433 MHz and 915 MHz. Complex transmission data are collected along and around the torso of a male subject. Full-wave numerical simulations and theoretical models are implemented based on simplified human torso model to provide physical insights into the experimental data [6]. Dynamic on-body propagation channels will also be briefly discussed [7].

Next we present a compact parasitic array design with potential on-body applications [8]. A four element array of folded cylindrical helix (FCH) is designed based on the identified dominant surface wave mechanism. The height and spacing of the array elements are carefully selected to maximize the array directivity. Both simulation and measurement results are presented.

II. WAVE PROPAGATION ALONG HUMAN BODY

A. Measurements

Fig. 1 shows the measurement setup. Both transmitting and receiving antennas are quarter-wavelength monopoles mounted on a small ground plane of a bridge shape. As the receiving antenna is moved away from the transmitting antenna over the torso of the male human subject (age 21 years, height 170 cm), complex transmission data (S_{21}) is recorded using a vector network analyzer (Agilent VNA N5230). The distance between the transceiving antennas ranges from 12 cm to 39 cm with a spacing of 3 cm.



Fig. 1. Along the torso S_{21} measurement

B. Analytical Model and Full Wave Simulation

Wave propagating along the human body can be approximately considered as the wave travelling along a planar lossy dielectric medium (Fig. 2). At high frequency, researchers have used a multi-layer model to represent for the biological tissues such as skin, bone, fat and muscle [2]. At lower frequency, as the wavelength becomes larger, we decide to use a single layer, homogeneous model with equivalent muscle tissue. The propagation mechanisms of an electric dipole antenna near an infinite ground plane have been investigated by Sommerfeld [9], whose theory is being utilized to solve for wave propagation along the human body for low frequencies.

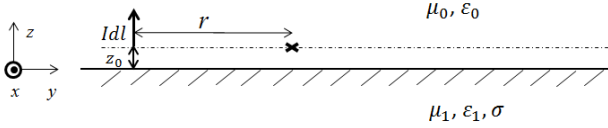


Fig. 2. Vertical electric current above a planar surface.

In Figure 2, the upper medium is the free space μ_0, ϵ_0 while the lower medium is the biological tissue $\mu_1, \epsilon_1, \sigma$. The propagation constants in the two media are $k^2 = k_0^2 = \omega^2 \mu_0 \epsilon_0$, $k_1^2 = k_0^2 \left(\epsilon_1 + j \frac{\sigma}{\omega \epsilon_0} \right)$. The complex index of refraction is defined as $n^2 = \epsilon_1 \left(1 + j \frac{\sigma}{\omega \epsilon_0} \right)$. For a z -directed infinitesimal dipole located at height z_0 , the electric field is expressed as [10]:

$$\bar{E} = -\frac{\omega \mu_0 I l}{4\pi k} \int_0^\infty d\lambda \frac{\lambda}{h} \begin{cases} \bar{N}_{e0\lambda}(h) [e^{-ihz_0} + b e^{ihz_0}] & z > z_0 \\ [\bar{N}_{e0\lambda}(-h) + b \bar{N}_{e0\lambda}(h)] e^{ihz_0} & 0 \leq z < z_0 \end{cases} \quad (1)$$

$$\text{Where } \bar{N}_{e0n\lambda}(h) = \frac{1}{\sqrt{\lambda^2 + h^2}}$$

$$\left[ih \frac{\partial J_n(\lambda r)}{\partial r} \frac{\cos n\theta \hat{r}}{\sin n\theta \hat{\phi}} \mp \frac{ihn}{r} J_n(\lambda r) \frac{\sin n\theta \hat{\theta}}{\cos n\theta \hat{\phi}} + \lambda^2 J_n(\lambda r) \frac{\cos n\theta \hat{z}}{\sin n\theta \hat{\phi}} \right] e^{ihz} \quad (2)$$

$$k^2 = h^2 + \lambda^2, \quad k_1^2 = h_1^2 + \lambda_1^2 \quad (3)$$

$$b = \frac{n^2 h - h_1}{n^2 h + h_1} \quad (4)$$

In our numerical example, the electric current source is placed at $z_0 = 1.5 \text{ cm}$, the observation point is located at $z = 1.7 \text{ cm}$, for $z > z_0$, the first integral formulation in (1) is used. λ is the free space wavelength and r is the distance from source (12 cm to 39 cm) along y axis. The lower medium is filled with equivalent muscle tissue with frequency dependent properties as listed in Table I [11]. The calculated normalized transmission loss and phase delay are shown in Figures 3(a) and (b) in solid lines. The black and red colors represent wave propagates at 433 MHz and 915 MHz, respectively.

TABLE I

HUMAN MUSCLE TISSUE PROPERTIES

Frequency (MHz)	433	915
Relative permittivity ϵ_1	56.873	54.997
Conductivity σ [S/m]	0.80484	0.84809

Full wave simulation is also performed in MOM based FEKO software to verify the analytical model. A monopole antenna (corresponding to the measurement setup) is placed 1.5 cm above on an infinite homogenous ground filled with muscle tissue property. The upper space is free space. The near electric field was collected 1.7 cm above the ground at every 3cm along the surface.

C. Results and Discussions

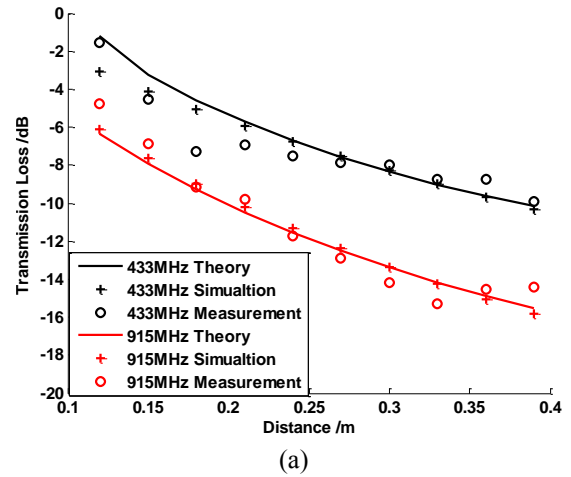
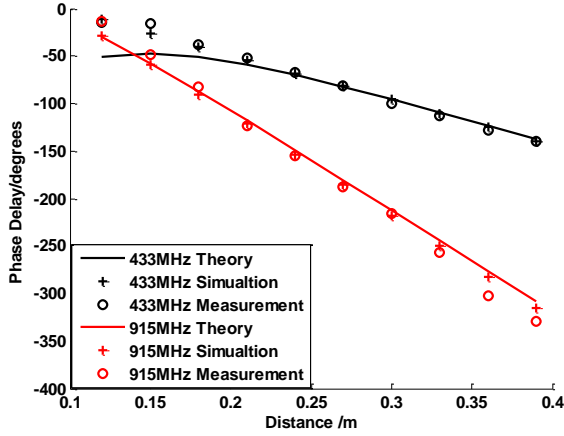


Fig. 3. LOS Comparison of measurement, simulation and analytical model for (a) transmission loss ([6])



(b)

Fig. 3. LOS Comparison of measurement, simulation and analytical model for (b) phase delay. ([6])

Figure 3 (a) shows the normalized transmission loss against distance (10 cm ~ 40 cm) at 433 MHz and 915 MHz. The analytical model shows good agreement with simulation and measurement at both frequencies. The discrepancies can be attributed to the different types of antennas: for theory, infinitesimal dipole is used; for simulation and measurement, the finite size monopole is used. Both antenna input impedance mismatch and antenna gain have been removed for a fair comparison. For the measurement and simulation of 433 MHz, the signal drops very fast in the first 17cm distance, due to the wave propagating in the near field region. In the theory result there is one smooth curve because it turns to all far fields in the whole range when the transmitter is an infinitesimal dipole. For 915 MHz, the signal strengths are 5dB weaker compared to 433 MHz.

The unwrapped phase delays in Figure 3 (b) show very good agreement between theory, simulation and measurement, except at the closer range in 433 MHz. The delay of phase is rather linear, indicating there is one dominant propagation mechanism with a unique travelling speed. β can be extracted using ESPRIT algorithm [5] and the results turn out to be 9.0087 radians/m for 433MHz, $19.7935 \text{ radians/m}$ for 915MHz, which are close to that in free space.

III. WAVE PROPAGATION AROUND HUMAN BODY

A. Measurements

Similar setup of the measurement is tested by VNA, as shown in Figure 4. The monopole antenna is fixed at the front center of the chest and the receiver is moved in a

horizontal level plane at every 1.5 cm around the torso. At each position, the complex transmission data (S_{21}) are recorded. During the measurement, the volunteer raises up both arms to avoid interference with propagation paths.



Fig. 4. Around the torso S_{21} measurement

B. Analytical Model and Full Wave Simulation

To help investigate wave propagation around the torso, we consider the wave propagation around the curvature of the human body. Several researchers have derived the analytical models with cylindrical [12] and elliptical [13] cylinder geometries at 2.45 GHz. For low frequency range, we apply Wait's theory to solve for wave travelling around the human body, as shown in the Figure 5. In [14], various modes contribute to the circumference attenuation rates known as creeping waves. For the vertical electric dipole source of moment Idl , the radial electric field intensity $|E_r|$ at a circle distance d is expressed as [15]:

$$\begin{aligned}
 E_r &= -\frac{jk_0 a Idl Z_0 \exp(-jk_0 a \theta)}{4\pi(r+h_1) d} e^{j(\omega_0 - \frac{\pi}{4})} 2(\sqrt{\pi x}) \\
 &\times \frac{e^{-jx t_1}}{t_1^0 - q^2} G(y_1) G(y_2) \\
 &- \frac{jk_0 a Idl Z_0 \exp(-jk_0 a \theta_c)}{4\pi(r+h_1) P-d} e^{j(\omega_0 - \frac{\pi}{4})} 2(\sqrt{\pi x_c}) \\
 &\times \frac{e^{-jx_c t_1}}{t_1^0 - q^2} G(y_1) G(y_2)
 \end{aligned} \quad (5)$$

where the circumference of the quasi-circle of the middle chest is P . $x = C\theta$ is the normalized range parameter. $x_c = C\theta_c$, $\theta_c = 2\pi - \theta$, $C = \sqrt[3]{\left(\frac{k_0 a}{2}\right)}$, $d = r\theta$. The normalized surface impedance $\Delta_0 = \sqrt{k_0/k_1 [1 - \left(\frac{k_0}{k_1}\right)^2 \sin^2 \theta]}$, $q = -jC\Delta_0$. $G(y) = \frac{w(t_1 - y)}{w(t_1)}$ is a 'height-gain' function, where $y_1 = \frac{k_0 h_1}{c}$, $y_2 = \frac{k_0 h_2}{c}$, h_1 and h_2 are the height of the dipole source and the observer. $w(t)$ is the Fock notation of the Airy function.

The roots \mathbf{t}_1^0 satisfy the boundary condition at the curved surface $\mathbf{w}' - \mathbf{q}\mathbf{w}(\mathbf{t}) = \mathbf{0}$.

For small value $|q| < |\mathbf{t}_1^0|$:

$$\mathbf{t}_1^0 = [0.375\pi]^{2/3} e^{-j\pi/3} \quad (6)$$

Where \mathbf{t}_1^0 represents the dominant creeping wave mode. Use (5) the normal component of electric field around the torso ($0 < \theta < 2\pi$) can be calculated. The source height h_1 and observation height h_2 are set 1.5 cm and 1.7 cm. The results are shown in Figures 6(a) and (b).

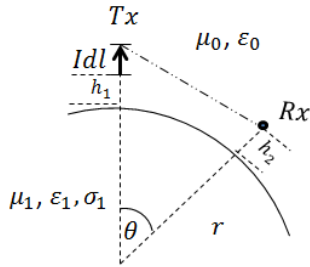


Fig. 5. Vertical electric dipole above a curve surface

Full wave simulation in FEKO is also performed for NLOS. The torso is modelled to be a finite height cylinder filled with homogeneous muscle tissue. The height and perimeter of the cylinder are 48.26 cm and 85.09 cm, corresponding to the height and perimeter of the test human object. The monopole antenna is placed in front of the middle level. Near electric fields are collected every 1.5cm at the same cross section level via probes.

C. Results and Discussions

Figures 6 (a) and (b) show NLOS theory, simulation and measurement comparisons at two frequencies. Among these frequency bands, good agreement can be clearly observed in both transmission loss and unwrapped phase delay. In Figure 6 (a), the transmission loss is plotted as a function of circumferential distance (3 ~ 82.5 cm) of the receiving antenna around the torso. The receiving field strength attenuates very fast as the receiving antenna is moved away from the transmitting antenna and drops to a constant level. As the receiving antenna is moved back to the front chest, the signal strength increases and returns to the initial level. This is because when the transmitter is fixed, two creeping waves propagate in opposite directions (i.e., clockwise and counter-clockwise) around the torso to the receiver. As the receiver is moved clockwise in the first half body circle,

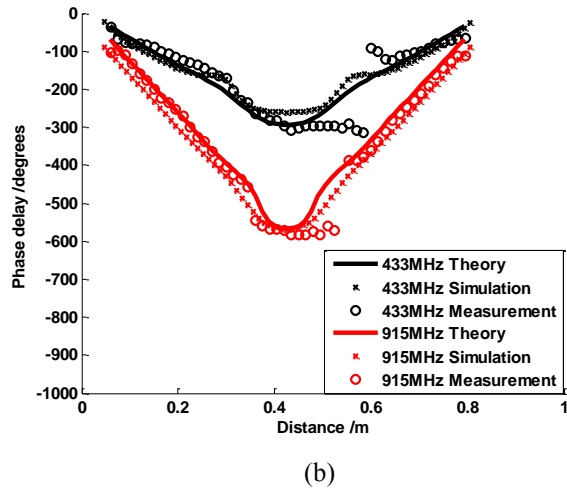
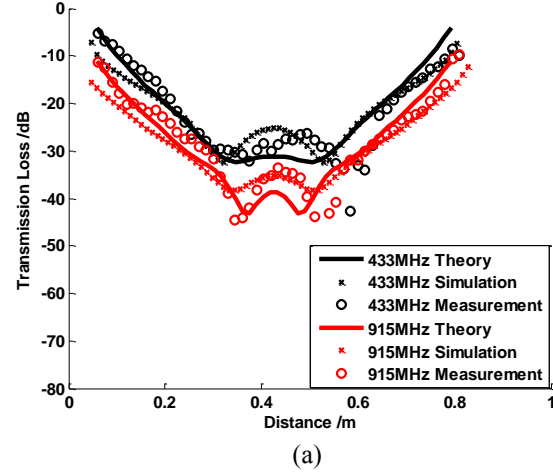


Fig. 6 NLOS Comparison of measurement, simulation and analytical model for (a) transmission loss (b) phase delay. ([6])

the dominant wave travels in the clockwise direction and signal drops as the distance increases. When the receiver is placed at the back, the waves from clockwise and counter-clockwise directions exhibit similar magnitudes and interfere with each other. As the receiver continues moving to the second half of the circle, the dominant wave switches to the counter clockwise path so the signal increases. The width of the region becomes narrower as the frequency goes higher, which is due to the weaker signal strength and smaller wavelength at higher frequency.

From the phase plot in the Figure 6 (b), the phase decreases linearly with increasing distance and goes flat when the receiver is at the back of the torso. It goes up linearly again as the receiver is moved back to the front chest. The extracted β values are 4.7454, -4.8421 radians /m for 433 MHz, and 19.8119, -19.4480 radians /m for 915 MHz, corresponding to waves travelling in opposite directions.

IV. DYNAMIC ON-BODY PROPAGATION

Recently, there is emerging interest in understanding how EM waves propagate on a dynamic moving human body and several numerical and experimental studies have been presented [16, 17]. Gallo [16] performed experiments with humans walking, and observed signal losses up to 10 fold, with even relatively small changes in body positions (e.g., an arm swinging) substantially affected signal strength. Hall [17] utilized a POSER walking model to simulate signal loss during dynamic motions.

To investigate how wireless transmission was perturbed due to body motions, a simple motion activity (one arm swinging along the side of a human body) was conducted and the wireless transmission data between the transmitting and receiving antennas was recorded [7]. The simulation results were compared with measurement data. Figure 7 (a) and (b) shows the experimental and simulation setup.

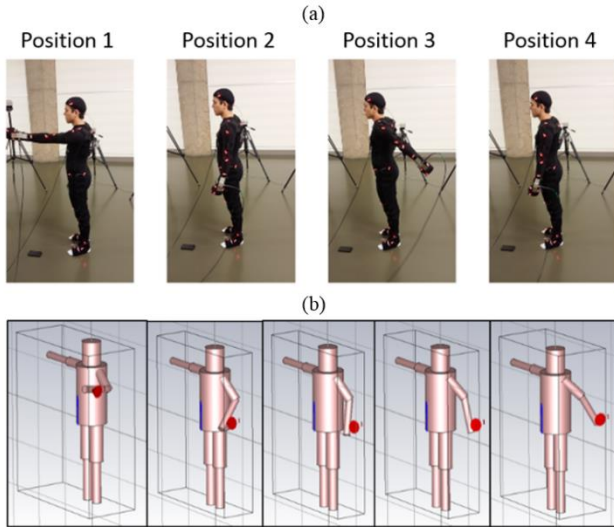


Fig. 7: (a) Experimental setup with volunteer wearing the 38-marker body suit and demonstrating the four second arm swing cycle. Approximately one second is taken between the shown arm positions. (b) Simulation setup of the left arm swing test represented in CST by 10-cylinder model at 433MHz. The red cone by the wrist represents the discrete port of the transmitting antenna. ([7])

Figure 8 shows a comparison at 433 MHz with the transmitting antenna at the left wrist with the receiving probe on the chest. It can be observed that both the simulation and experiment have periodic patterns with the same time interval as the motion pattern. It can also be observed that the signal strength is lower when the arm is alongside the body compared to when it is either in front of the body (shoulder flexion) or behind the body (

shoulder extension). The simulation and experiment show decent agreement in terms of amplitude, period, and shape, but there are discrepancies when the arm is in front of the body. A possible source of this difference is that the simulation model did not include environmental obstacles such as the floor and the walls.

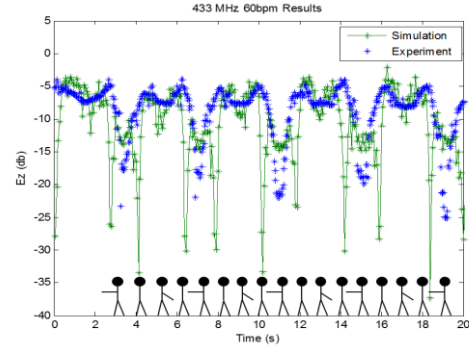


Fig. 8. Measured and Simulated S_{21} data at 433 MHz over 4 cycles of arm swing motion with transmitter on wrist and probe on chest. ([7])

V. COMPACT ANTENNA ARRAY DESIGN

Finally, a compact size, low-profile parasitic surface wave antenna array design was presented for potential on-body applications [8]. Figure 9 plots the array design setup, which consists of four folded cylindrical helix (FCH) elements. The design frequency is at 400 MHz. The total length of the array is assumed to be $0.5 \lambda_0$, where λ_0 is the free space wavelength.

Given this fixed array size, the propagation constant of the surface wave has to be carefully determined to maximize the directivity of the array, which is similar to the 1-D metal wire antenna array design [18]. The optimum phase constant β_{opt} for this half wavelength array is found to be $-1.98 k_0$. Then the radius R , height H , and spacing S are selected to be 3.12 cm, 4.9 cm and 10.4 cm to achieve this β_{opt} .

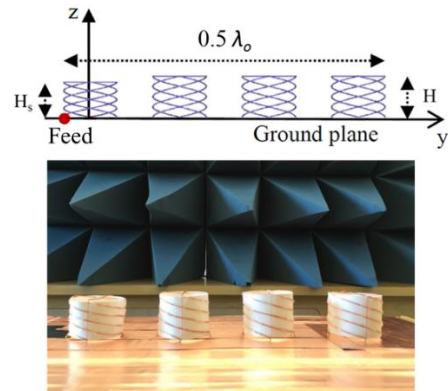


Fig. 9. 1-D closely-spaced, low-profile antenna array. ([8])

Figure 10 shows the antenna reflection coefficients versus frequency. The center resonance frequencies are found to be 400 MHz and 386 MHz for simulation and measurement. The -10dB bandwidths are both 3 MHz. Figure 11 compares the simulated and measured gain in the backward endfire direction ($\theta=90^\circ$, $\phi=270^\circ$). The maximum gain values are 10.99 dBi for simulation and 10.33 dBi for measurement. Finally, Figure 12 plots the simulated antenna array radiation patterns in the azimuth plane ($\theta=90^\circ$) at the center frequency. The simulated and measured front-to-back ratio are found to be 9.4 and 12.8 dB.

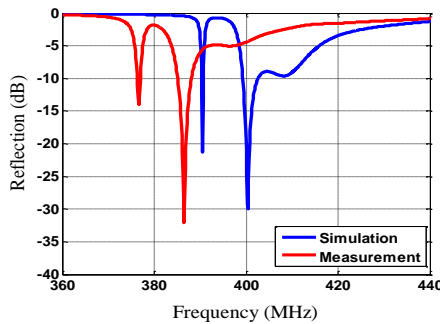


Fig. 10 Simulated and measured reflection coefficients. ([8])

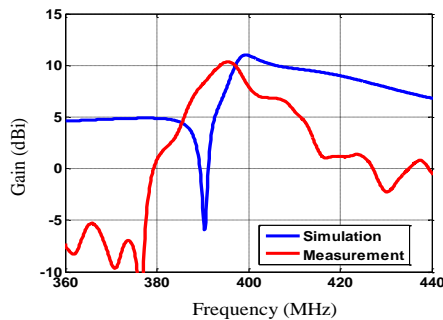


Fig. 11 Simulated and measured antenna gain ([8])

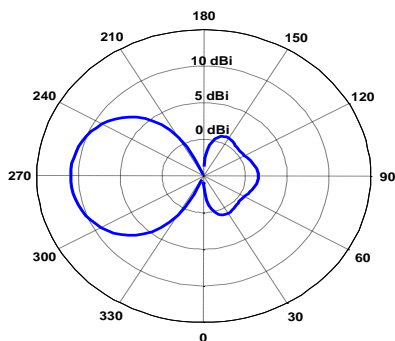


Fig. 12 Simulated radiation pattern in the azimuth plane ([8])

VI. CONCLUSION

In this work the on-body wave propagations are studied in lower UHF frequency bands of 433 MHz and 915 MHz. Wave propagation along the body can be modelled as ground wave propagation on an infinite large ground. Wave propagation around the human can be considered as creeping wave around a cylinder. The analytical models based on theories are derived and verified through simulations and measurements. The dynamic on-body wave propagation was illustrated, and a compact size, low profile surface antenna array was presented.

REFERENCE

- [1] H. Cao, V. Leung, C. Chow, and H. Chan, "Enabling technologies for wireless body area networks: a survey and outlook," *IEEE Commun. Mag.*, vol. 47, no. 12, pp.84 -93, Dec. 2009.
- [2] P. S. Hall, Y. Hao, Y. I. Nechayev, A. Alomainy, C. C. Constantinou, C. Parini, M. R. Kamarudin, T. Z. Salim, D. T. M. Hee, R. Dubrovka, A. S. Owadally, W. Song, A. Serra, P. Nepa, and M. Gallo, "Antennas and propagation for on-body communication systems," *IEEE Antenna Propag. Mag.*, vol. 49, no. 3, pp. 41–58, Jun. 2007.
- [3] D. Smith, D. Miniutti, T. Lamahewa, and L. Hanlen "Propagation models for body-area networks: A survey and new outlook," *IEEE Antennas Propag. Mag.*, vol. 55, no. 5, pp.97 -117, May 2013.
- [4] D. Xue, B. Garner, and Y. Li, "Investigation of short-range, broadband, on-body electromagnetic wave propagations," *IET Microwaves Antennas Propagat.*, submitted for publication.
- [5] D. Xue, B. Garner, and Y. Li, "Extraction of on-body creeping wave mechanism using the ESPRIT algorithm," *Microwave Optical Tech. Lett.*, vol. 57, no. 4, pp. 868–871, Apr. 2015.
- [6] D. Xue, B. Garner and Y. Li, "Investigation of 433 MHz and 915 MHz on-body wave propagations," *IEEE MTT 2015 Texas Symposium on Microwave and Wireless Circuits and Systems*, Waco, TX, Apr. 2015.
- [7] A. Hoeckel, G. Lee, E. Forrister, D. Xue, B. Garner, G. Benton and Y. Li, "Simulation and measurement of dynamic on-body wave propagations," *IEEE MTT 2015 Texas Symposium on Microwave and Wireless Circuits and Systems*, Waco, TX, Apr. 2015.
- [8] B. Xu and Y. Li, "Backward surface wave propagation and radiation along a one-dimensional folded cylindrical helix array," *International Journal of Antennas and Propagation*, Article ID 210254, 9 pages, 2015.
- [9] A. Sommerfeld, "Über die Ausbreitung der Wellen in der drahtlosen Telegraphie," *Annalen der Physik*, vol. 28, pp. 665, 1909.
- [10] P. M. Hansen, "The radiation efficiency of a dipole antenna above an imperfectly conducting ground," PhD dissertation, 1970.
- [11] Internet resource for dielectric human tissue properties. <http://niremf.ifac.cnr.it/tissprop/htmlclie/htmlclie.htm#atsfta>

- [12] T. Alves, B. Poussot and J. Laheurte, "Analytical propagation modelling of BAN channels based on the Creeping-Wave theory," *IEEE Trans. On Antennas and Propagation*, vol. 59, no. 4, pp. 1269-1274, April 2011.
- [13] R. Chandra and A. J. Johansson, "An elliptical analytical link loss model for wireless propagation around the human torso," *6th European Conference on Antennas and Propagation*, 2011.
- [14] J. R. Wait, "On the excitation of electromagnetic surface wave on a curved surface," *IRE Transactions on Antennas and Propagation*, vol. 8, no. 4, pp. 445-448, July 1960.
- [15] G. A. Conway, W.G. Scalon, S.L. Cotton, and M.J. Bantum, "An analytical path-loss model for on-body radio propagation," *URSI International Symposium on Electromagnetic Theory*, August 2010.
- [16] M. Gallo, P. S. Hall, Y.I. Nechayev and M. Bozzetti, "Use of animation software in simulation of on-body communications channels at 2.45GHz," *IEEE Antennas and Wireless Propag. Lett.*, vol. 7, pp. 321-324, October 2008.
- [17] Hall, P S and Hao, Y, (editors) "Antennas and Propagation for Body Centric Communications Systems", (Artech House, Norwood, MA, USA, 2012, 2nd edition, ISBN-13: 978-1608073764
- [18] D. Xue and Y. Li, "Design of a closely-spaced, multiple-element parasitic antenna array," *Microwave Optical Tech. Lett.*, vol. 56, no. 10, pp. 2374-2377, Oct. 2014.



Yang Li received his B.S. degree in electrical engineering from the University of Science and Technology of China, in 2005, and his M.S and Ph.D. degrees in electrical and computer engineering from the University of Texas at Austin, in 2007 and 2011,

respectively. He joined the faculty of the Baylor University in August 2011 and is currently an Assistant Professor of Electrical and Computer Engineering department.

Dr. Li's research interests include body area wave propagation and antenna radiation, effective medium theory and homogenization technique, electrically small antenna design, leaky-wave antenna design, micro-doppler radar and metamaterials.

He is the recipient of a Young Scientist Award from URSI, the CST university publication award, the Doctoral Research Award from the IEEE Antennas and Propagation Society, the 3rd prize at the 2010 USNC-URSI National Radio Science Meeting paper contest, and the Houston Endowment President's Excellence Fellowship from the University of Texas at Austin.